Inorg. Chem. **1999,** *38,* 744−750

Kinetics and Mechanisms of Reactions of Alkyl Hydroperoxides with Methylrhenium Oxides

Kimberly A. Brittingham and James H. Espenson*

Iowa State University, 25 Spedding Hall, Ames, IA 50011

Received July 30, 1998

Aqueous methyldioxorhenium (MDO), prepared from methyltrioxorhenium (MTO) and hypophosphorous acid, abstracts an oxygen atom from tertiary alkyl hydroperoxides. This regenerates MTO and forms the tertiary alcohol with rate constants 3.71×10^4 L mol^{-1} s^{-1} (*t*-BuOOH) and 3.47×10^4 L mol^{-1} s^{-1} (*t*-AmOOH) at 25.0 °C in aqueous 1.0 M HOTf. MDO reacts with hydrogen peroxide first to form MTO, $k = 3.36 \times 10^4$ L mol^{-1} s^{-1}, which subsequently reacts with more hydrogen peroxide to form peroxorhenium complexes. In a separate study, the concomitant slow decomposition of alkyl hydroperoxides and MTO (to ReO_4^-) was investigated. The rate law is v = k[MTO][$RCMe_2OOH$]/[H^+], with $k = 7.4 \times 10^{-5}$ s^{-1} (R = Me) and $k = 8.4 \times 10^{-5}$ s^{-1} (R = Et) at 25.0 °C in aqueous solution at μ 1.0 M. ^{1}H NMR spectroscopy and GC revealed organic products suggestive of radical reactions. The products from *t*-BuOOH are acetone, methanol, *tert*-butyl methyl ether, methane, ethane, and *tert*-butyl methyl peroxide. With CH_2DReO_3, it could be shown that both *t*-BuOOH and MTO were sources of the methane. The rate of decomposition of MTO shows an inverse-first-order dependence on [H^+] throughout the range pH 1−6.42.

Introduction

An extensive amount of literature now describes how hydrogen peroxide and MTO (CH_3ReO_3) form η^2-peroxorhenium species, **A** = $CH_3Re(\eta^2\text{-}O_2)(O)_2$ and **B** = $CH_3Re(\eta^2\text{-}O_2)_2(O)(H_2O)$, eq 1.[1−4] Both are active catalysts for hydrogen peroxide oxidations.[5]

$$CH_3ReO_3 \underset{H_2O}{\overset{H_2O_2}{\rightleftharpoons}} CH_3Re(\eta^2\text{-}O_2)(O)_2\ (\mathbf{A}) \overset{H_2O_2}{\rightleftharpoons} CH_3Re(\eta^2\text{-}O_2)_2O(H_2O) \quad (1)$$

In solutions containing hydrogen peroxide, MTO is prone to irreversible decomposition by the nucleophilic hydroperoxide anion, HO_2^- (eq 2)[6] and OH^- (eq 3).[6,7]

$$HO_2^- + CH_3ReO_3 \rightarrow CH_3OH + ReO_4^- \quad (2)$$

$$OH^- + CH_3ReO_3 \rightarrow CH_4 + ReO_4^- \quad (3)$$

The rhenium(V) compound methyldioxorhenium (MDO, solvated or ligated) abstracts an oxygen atom from many oxygen donors XO:[7−9] XO + CH_3ReO_2 → X + CH_3ReO_3, driven by the strength of the rhenium−oxygen bond in MTO, 464 kJ mol^{-1}.[9] Hydrogen peroxide converts MDO into the peroxo complexes **A** and **B**. Alkyl hydroperoxides, on the other hand, yield only MTO, allowing a kinetic analysis of the first stage:

$$ROOH + CH_3ReO_2 \rightarrow ROH + CH_3ReO_3\ (k_4) \quad (4)$$

The slow decomposition of CH_3ReO_3 in aqueous solutions containing Me_3COOH (*t*-BuOOH) or $EtCMe_2OOH$ (*t*-AmOOH) has been studied. The different rhenium and organic products were used to assign a mechanism that clearly involves free radicals. Cumyl hydroperoxide, $C_6H_5(CH_3)_2COOH$, is decomposed heterolytically by MTO in chlorobenzene; <1% of the process involves radicals.[10]

Experimental Section

Materials. A Millipore-Q water-purification system provided high-purity water. Deuterium oxide (99%) was used as the NMR solvent. Solutions were acidified with trifluoromethanesulfonic acid (HOTf, triflic acid) diluted from the commercially available material (98%). Perchloric acid or its salts could not be present, owing to the reaction between MDO and ClO_4^-.[8] Where needed, ionic strength was maintained with lithium triflate.

t-Butyl hydroperoxide was obtained commercially as a 70% solution in water. *t*-Amyl hydroperoxide was synthesized and analyzed as previously described.[11] CH_2DReO_3 was synthesized from dirhenium heptoxide, trifluoroacetic acid, and $CH_2DSn(n\text{-butyl})_3$,[12] kindly donated by Dr. Michael T. Ashby. Other reagents were available commercially: MTO, hypophosphorous acid (50% in water), phosphorous acid, *tert*-butyl alcohol, hydrogen peroxide (30% in water), *t*-amyl alcohol, 2-methyl-1-phenyl-2-propanol, HPLC grade acetonitrile, dirhenium heptoxide, and trifluoroacetic acid. Methyldioxorhenium (MDO)

---

(1) Herrmann, W. A.; Fischer, R. W.; Scherer, W.; Rauch, M. U. *Angew. Chem., Int. Ed. Engl.* **1993**, *32*, 1157.
(2) Yamazaki, S.; Espenson, J. H.; Huston, P. *Inorg. Chem.* **1993**, *32*, 4683.
(3) Espenson, J. H.; Pestovsky, O.; Huston, P.; Staudt, S. *J. Am. Chem. Soc.* **1994**, *116*, 2869.
(4) Hansen, P. J.; Espenson, J. H. *Inorg. Chem.* **1995**, *34*, 5839.
(5) Espenson, J. H.; Abu-Omar, M. M. *Adv. Chem. Ser.* **1997**, *253*, 99−134.
(6) Abu-Omar, M. M.; Hansen, P. J.; Espenson, J. H. *J. Am. Chem. Soc.* **1996**, *118*, 4966.
(7) Zhu, Z.; Espenson, J. H. *J. Mol. Catal.* **1995**, *103*, 87.
(8) Abu-Omar, M. M.; Espenson, J. H. *Inorg. Chem.* **1995**, *34*, 6239.
(9) Abu-Omar, M. M.; Appleman, E. H.; Espenson, J. H. *Inorg. Chem.* **1996**, *35*, 7751.
(10) Smurova, L. A.; Kholopov, A. B.; Nikitin, A. V.; Brin, E. F.; Rubailo, V. L. *Kinet. Catal. (Transl. of Kinet. Katal.)* **1996**, *37*, 361.
(11) Leslie, J. P., II.; Espenson, J. H. *J. Am. Chem. Soc.* **1976**, *98*, 4839.
(12) Herrmann, W. A.; Kühn, F. E.; Fischer, R. W.; Thiel, W. R.; Romão, C. C. *Inorg. Chem.* **1992**, *31*, 4431.

10.1021/ic9809052 CCC: $18.00

was generated in situ from hypophosphorous acid and MTO in strongly acidic aqueous solution, $k_5 = 2.8 \times 10^{-2}$ L mol^{-1} s^{-1} at 25.0 °C:[9]

$$CH_3ReO_3 + H_3PO_2 \rightarrow CH_3ReO_3 + H_3PO_3\ (k_5) \qquad (5)$$

With higher (∼10 mM) concentrations of MDO for NMR studies, a blue color indicated the onset of MDO oligomerization.[8,9] The addition of alkyl hydroperoxide immediately restored colorless MTO. We surmise that the disappearance of oligomer in this case is analogous to perchlorate reduction by dimeric MDO.[8] Oligomerization might have been largely avoided by maintaining pH 0, but this was not feasible because of NMR shimming difficulties.

Instrumentation. Spectrophotometric data were recorded using Shimadzu UV-2501PC and UV-3101PC spectrophotometers. Kinetic data for fast reactions were collected with an Applied Photophysics Sequential DS-17MV stopped-flow spectrophotometer. ^{1}H NMR spectra, used to monitor MTO (s, 2.46 ppm) and organic products over time in D_2O, were obtained with Varian VXR-300 or Bruker DRX-400 spectrometers. Acetonitrile was the internal standard (δ 2.09 ppm). ^{31}P chemical shifts were referenced to 85% H_3PO_4. ^{1}H NMR kinetics were recorded with the Bruker spectrometer at 22.5 ± 0.2 °C. The chemical shifts of the proton resonances for the organic reactants and products are as follows:

$(C\mathit{H}_3)_2CO$ δ 2.25 (s, 6H)
$(C\mathit{H}_3)_3COH$ δ 1.271 (s, 9H)
$(CH_3)_3COC\mathit{H}_3$ δ 3.25 (s, 3H)
$C\mathit{H}_3OOH$ δ 3.887 (s, 3H)
$(C\mathit{H}_3)_3COOH$ δ 1.266 (s, 9H)
$C\mathit{H}_3OH$ δ 3.37 (s, 3H)
$(CH_3)_3COOC\mathit{H}_3$ δ 3.86 (s, 3H)
$C\mathit{H}_2O$ δ 5.092 (s, 2H)
$C\mathit{H}_3CH_2(CH_3)_2COOH$ δ 0.893 (t, 3H)
$CH_3C\mathit{H}_2(CH_3)_2COOH$ δ 1.601 (q, 2H)
$CH_3CH_2(C\mathit{H}_3)_2COOH$ δ 1.215 (s, 6H)
$C\mathit{H}_3CH_2(CH_3)_2COH$ δ 0.86 (t, 3H)
$CH_3C\mathit{H}_2(CH_3)_2COH$ δ 1.485 (q, 2H)
$CH_3CH_2(C\mathit{H}_3)^2COH$ δ 1.166 (s, 6H)
$CH_3CH_2(CH_3)_2COC\mathit{H}_3$ δ 3.217 (s, 3H)
$CH_3CH_2(CH_3)_2COOC\mathit{H}_2CH_3$ δ 3.678 (q, 2H)

The chemical shifts for the commercially available compounds were assigned on the basis of authentic samples. The CH_3OOH was prepared by literature methods.[13] The $(CH_3)_3COOCH_3$ was prepared from dimethyl sulfate and *tert*-butyl hydroperoxide on the basis of the same procedure.[13] A quartet resonance among the products of the reaction of *t*-AmOOH and MTO is the result of an unassigned methylene group of an ethyl group that has been shifted downfield by an oxygen. We take this resonance to be that of *t*-amyl ethyl peroxide because the *t*-BuOOH reaction forms the analogous dialkyl peroxide.

Methane, ethane, ethylene, and propane were detected by gas chromatography on a VZ-10 column. Perrhenate ions were detected with a Perkin-Elmer Sciex API electrospray mass spectrometer with a syringe injector. GC−MS experiments were performed with a TSQ700 mass spectrometer (Finnigan MAT). The mass spectra were obtained by scanning the first quadrupole from *m*/*z* 10 to *m*/*z* 20 for 0.5 s. The second and third quadrupoles were maintained in the RF only mode. The system was configured in the electron impact ionization mode. A DB1 column was used. The injector and transfer-line temperatures were maintained at 260 and 240 °C, respectively.

Results

Kinetics of the Reaction of MDO with ROOH. Kinetic data were obtained with the stopped-flow technique at 25.0 ± 0.2 °C in aqueous solution. The MDO solution was prepared from MTO and hypophosphorous acid in one of the SF syringes containing HOTf and/or LiOTf. After 5 half-lives for MDO formation had elapsed, $k_5 = (2.8 \pm 0.2) \times 10^{-2}$ L mol^{-1} s^{-1}, the MDO solution was mixed in the SF apparatus with the contents of the other syringe holding the appropriate concentrations of ROOH, HOTf, and LiOTf. The buildup of MTO was monitored at 270 nm (ϵ = 1300 L mol^{-1} cm^{-1}). The reactant concentrations were varied over these ranges: 50−200 μM MDO and 0.5−10 mM *t*-BuOOH. In addition, the concentrations of H_3PO_2 and H$^+$ were varied modestly, 0.05−0.1 M and 0.032−1.0 M, respectively, to confirm the absence of kinetic effects from these variables. Ionic strength was maintained at 1.0 M with lithium triflate. The absorbance−time data in each experiment were fit to first-order kinetics, eq 6, since the alkyl hydroperoxide was taken in substantial excess.

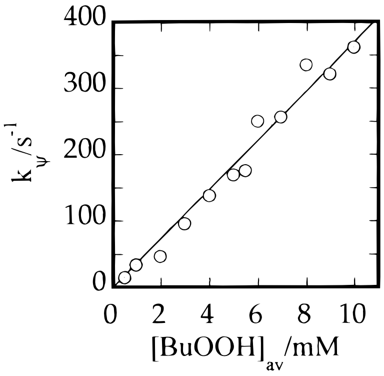

Figure 1. Kinetic data for the reaction of *tert*-butyl hydroperoxide with methyldioxorhenium in aqueous solutions of triflic acid (0−1.0 M) at 25.0 °C and ionic strength 1.0 M. Shown is a plot of the pseudo-first-order rate constant against the average concentration of the hydroperoxide, the reagent in excess.

$$\mathrm{Abs}_t = \mathrm{Abs}_\infty + (\mathrm{Abs}_0 - \mathrm{Abs}_\infty)e^{-k_\psi t} \qquad (6)$$

The variation of k_ψ with [*t*-BuOOH]$_{av}$ is presented in Figure 1. A linear least-squares fit gave k_4 at 25.0 °C as the slope: (3.71 ± 0.10) × 10^4 L mol^{-1} s^{-1}. For *t*-AmOOH, $k_4 = (3.47 \pm 0.07) \times 10^4$ L mol^{-1} s^{-1}.

The reactions in eqs 4 and 5 constitute a catalytic cycle, the faster step destroying MDO and the other reforming it more slowly. In effect, then, MTO catalyzes the reaction between hypophosphorous acid and alkyl hydroperoxide:

$$ROOH + H_3PO_2 \xrightarrow{\text{cat. MTO}} ROH + H_3PO_3 \qquad (7)$$

This is a spontaneous reaction in the thermodynamic sense, but it does not occur under these conditions without a catalyst. In the course of checking the catalytic reaction, other reactions were found to take place concurrently over longer times (here limited by the lower rate of reaction 5). The additional reactions entailed the concurrent decomposition of MTO and ROOH, as discussed later.

Kinetics of the Reaction of MDO with H_2O_2. In principle, these experiments were the same as those just reported for ROOH, except that reaction 4 is followed by others, leading to further products, eq 1. When MDO ([MTO]$_0$ = 0.1 mM, [H_3PO_2]$_0$ = 50 mM) was mixed with H_2O_2 (10 mM), the absorbance at 270 nm for MTO increased with time according to first-order kinetics. For that stage, the rate constant for the reaction between MDO and H_2O_2 is $k_4 = (3.36 \pm 0.02) \times 10^4$ L mol^{-1} s^{-1}. Over longer times, the formation of **B** was monitored at 360 nm. The pseudo-first-order rate constant of this second component agreed with that determined directly for H_2O_2 + MTO. These findings provide spectroscopic and kinetic evidence that MTO was formed in the first step.

Kinetics of the Concurrent Decomposition of MTO and $RCMe_2OOH$. In the strongly acidic medium needed to stabilize MDO, pH 0−1, MTO remains fairly stable without the hydroperoxide. With hydroperoxide, however, both MTO and the alkyl hydroperoxide slowly decompose *concurrently* at a pH dependent rate.

---

(13) Davies, D. M.; Deary, M. E. *J. Chem. Soc., Perkin Trans. 2* **1992**, 559.

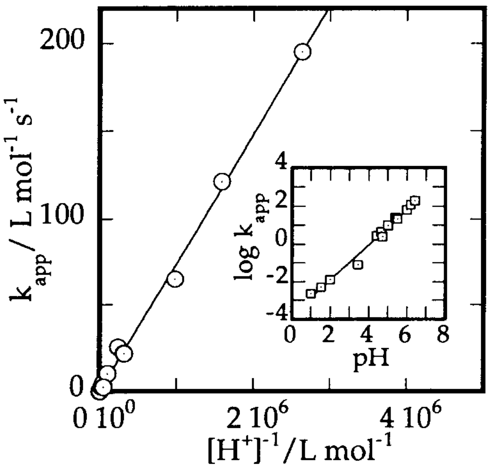

Figure 2. Dependence of second-order rate constant, k_{app}, on $1/[H^+]$ at 25 °C. Slope is $k_f = (7.4 \pm 0.1) \times 10^{-5}$ s^{-1}. Inset shows a plot of log k vs pH, with a slope 0.93 ± 0.03. Points at pH 1, 2, 3.44, and 4.72 were at $\mu = 1.0$ M; the others were at $\mu = 0.05$ M.

The decomposition of MTO (0.5 mM) by $RCMe_2OOH$ (10 mM) was monitored spectrophotometrically at 270 nm at pH 1.0−6.42. The data were fit to first-order kinetics at each pH. Values of an apparent second-order rate constant were calculated as $k_{app} = k_\psi/[RCMe_2OOH]$. The plot of log k_{app} versus pH was linear, Figure 2 inset, with a slope of 0.93 ± 0.03. Thus, the decomposition is inverse-first-order with respect to $[H^+]$. Reactions of *t*-AmOOH were monitored at pH 1, 2, and 3.25. The pattern closely resembles that of *t*-BuOOH. The rate equation for both is

$$v = k_f \frac{[MTO][RCMe_2OOH]}{[H^+]} \tag{8}$$

The plot of k_{app} versus $1/[H^+]$ is linear, Figure 2. The data in this plot were taken from experiments at ionic strengths of 0.05 and 1.0 M. The k_f values from these fits are $(7.4 \pm 0.1) \times 10^{-5}$ s^{-1} (*t*-BuOOH) and $(8.4 \pm 0.4) \times 10^{-5}$ s^{-1} (*t*-AmOOH) at 25.0 °C.

^{1}H NMR was used to study the dependence of the same reaction ($\mu = 0.1$ M, $[H^+] = 0.1$ M) on [*tert*-BuOOH] at 22.5 °C. The values of k_ψ for the disappearance of MTO were plotted against [*t*-BuOOH] to give $k_{app} = (2.41 \pm 0.07) \times 10^{-4}$ L mol^{-1} s^{-1}, where $k_{app} = k_f/[H^+]$. Therefore, according to these NMR experiments, $k_f = (2.41 \pm 0.07) \times 10^{-5}$ s^{-1}. These values for k_f, as determined by UV−vis spectrophotometry and NMR, differ by a factor of 3. This discrepancy arises from the use of quite different ranges of reactant concentrations, a different experimental technique, a different reaction medium, and a modestly different temperature.

Products of Decomposition of MTO and *t*-BuOOH. The decomposition of MTO and *t*-BuOOH might be anticipated to parallel reaction 2. Perrhenate ions and *tert*-butyl methyl ether would be the products from attack of the *tert*-butyl peroxide anion on MTO. These products were indeed found, but others were formed as well. The loss of MTO and *t*-BuOOH under an Ar atmosphere was monitored by NMR. GC was also employed to detect alkanes in the gas phase. The products included $(CH_3)_2CO$, CH_3OH, *t*-$BuOCH_3$, CH_4, C_2H_6, and *t*-$BuOOCH_3$. Although *t*-BuOH is seen as a product by ^{1}H NMR, its signal overlaps that for *t*-BuOOH, and therefore the change in its peak intensity could not be monitored. The perrhenate ion was also qualitatively detected using electrospray mass spectroscopy. The initial concentrations were: ~10 mM MTO, 200 mM *t*-BuOOH, 100 mM HOTf, and 10 mM CH_3CN as the NMR standard. The reagents were added except *t*-BuOOH, and the NMR spectrum recorded. Then *t*-BuOOH was added and the spectrum recorded over approximately 4 h. The concentration−time data for the decrease in MTO and the increase in reaction products were fit to first-order kinetics. The rate constants are reported in Table 1.

Table 1. Rate Constants for the Decrease of MTO and Increase of Products During the Decomposition of MTO (17 mM) and *t*-BuOOH (200 mM) at 22.5 ± 0.2 °C

species	$k_{dec}/10^{-5}$ s^{-1}	final concn^a/mM
MTO	6.2 ± 0.2	0.4 ± 0.1
CH_3OH	5.55 ± 0.07	4.44 ± 0.02 (26%)^b
$(CH_3)_2CO$	6.1 ± 0.1	2.78 ± 0.2 (16%)
t-$BuOCH_3$	5.9 ± 0.1	2.37 ± 0.02 (14%)
t-$BuOOCH_3$	5.2 ± 0.2	1.85 ± 0.04 (11%)

[a] From least-squares fitting of the experimental data. [b] Percent yield relative to $[MTO]_0$.

According to Table 1, the pseudo-first-order rate constants for the decomposition of MTO and the buildup of methanol, acetone, *tert*-butyl methyl ether, and *tert*-butyl methyl peroxide are the same within error. The weighted mean[14] of these first-order rate constants is $k_{dec} = (5.76 \pm 0.05) \times 10^{-5}$ s^{-1}. Table 1 also reports the final concentration of each product. It is difficult to calculate the mass balance of products because of the complicated radical decomposition process, which is discussed later.

Methane and ethane were monitored by gas chromatography. MTO (10 mM) and *t*-BuOOH (200 mM) were mixed together in 0.1 M HOTf at room temperature. The total volume of solution was 7 mL. The reaction was carried out in a 20-mL bottle sealed with a septum. No care was taken to exclude oxygen. The solution was shaken vigorously, and then the headspace was injected into the GC. Data seemed to indicate that the these products were formed much faster than those detected by NMR spectroscopy. It should be noted that these experiments were done to detect methane and ethane and are of qualitative significance only.

To determine whether MTO or *t*-BuOOH or both were a source of Me$^\bullet$, 98% CH_2DReO_3 was employed. The GC of the argon-saturated solution indicated peaks for methane and water. The MS of the methane peak showed a significant amount of the CH_3D^+ ion at *m*/*z* 17. It was not possible to determine the ratio CH_3D/CH_4 to sufficient accuracy, but it was evident that both were present. Thus, the methane is composed of methyl radical that is partly derived from the β-scission of the *tert*-butoxyl radical and partly from MTO decomposition.

Products of the Decomposition of MTO and *t*-AmOOH. Acetone, methanol, *t*-amyl methyl ether, and *t*-amyl ethyl peroxide were detected by ^{1}H NMR. The rate constants, k_{dec}, for the decrease in MTO and increase in organic products, Table 2, show a weighted mean[14] of $(2.36 \pm 0.04) \times 10^{-4}$ s^{-1}.

Gaseous products, namely methane, ethane, ethylene, and propane, were detected by GC. Methane was formed in a higher yield than ethane. Ethylene and propane were minor. Quantitative statements cannot be made.

Experiments in the Presence of Oxygen. The reaction between MTO (10 mM) and *t*-BuOOH (200 mM) under O_2 gave two additional organic products, methyl hydroperoxide and formaldehyde.

---

(14) Bevington, P. R.; Robinson, D. K. *Data Reduction and Error Analysis for the Physical Sciences*. 2nd ed.; McGraw-Hill: St. Louis, 1992.

Table 2. Rate Constants for the Decrease of MTO and Increase of Products During the Decomposition of MTO (7.0 mM) and *t*-AmOOH (200 mM) at 22.5 ± 0.2 °C

species	$k_{dec}/10^{-4}\ s^{-1}$	final concn[a]/mM
MTO	2.13 ± 0.08	1.2 ± 0.1
CH_{3OH}	2.53 ± 0.07	3.89 ± 0.05 (56%)[b]
$(CH_3)_2CO$	1.7 ± 0.2	5.21 ± 0.05 (74%)
t-$AmOCH_3$	2.59 ± 0.07	0.83 ± 0.02 (12%)
t-$AmOOCH_2CH_3$	1.3 ± 0.2	4.0 ± 0.7 (57%)

[a] From least-squares fitting of the experimental data. [b] Percent yield relative to $[MTO]_0$.

Table 3. Rate Constants and Final Concentrations for the Decomposition of MTO and the Buildup of Products in the Reaction of MTO (10 mM), H_3PO_2 (100 mM), and *t*-BuOOH (200 mM) at 22.5 ± 0.2 °C[a]

species	$k_{dec}/10^{-5}\ s^{-1}$	final concn[b]/mM
MTO	15 ± 2	4.3 ± 0.2
CH_3OH	17.1 ± 0.8	3.84 ± 0.05 (38%)[c]
$(CH_3)_2CO$	50 ± 2	73 ± 2 (730%)
t-$BuOCH_3$	9.4 ± 0.7	0.88 ± 0.02 (9%)
t-$BuOOCH_3$	54 ± 1	2.46 ± 0.03 (25%)

[a] $[HOTf]_0 = 100$ mM. [b] From least-squares fitting of the experimental data. [c] Percent yield relative to $[MTO]_0$.

Phosphoric Acid. No conditions have been found under which H_3PO_2 or H_3PO_3 could be oxidized to phosphate by MTO catalyzed reactions of hydrogen peroxide. To our surprise then, phosphoric acid was produced when *t*-BuOOH was added to a solution of MDO containing excess H_3PO_2. This experiment consisted of adding 200 mM *t*-BuOOH to a solution prepared from 10 mM MTO and 100 mM H_3PO_2 that had been allowed to stand for 88 s, in which time the blue color for MDO oligomerization became apparent. The ^{31}P NMR spectrum of this reaction mixture was used to substantiate H_3PO_3 (d, 5.49 ppm) and H_3PO_4 (s, 0.63 ppm).

Under these conditions, hypophosphorous acid and *tert*-butyl hydroperoxide do not react without MTO. Phosphoric acid was formed at approximately the same rate when H_3PO_2 was replaced by H_3PO_3. When chlorate ion, ClO_3^-, was used in place of *t*-BuOOH, phosphorous acid was the only product. These findings suggest that the precursor to phosphoric acid is phosphorous acid. Also, phosphoric acid formation is probably due to radical processes occurring in the *t*-BuOOH system because the effect was absent with ClO_3^-.

The rate constants for MTO loss and product buildup are given in Table 3. The weighted mean[14] of the rate constants for the loss of MTO and the buildup of methanol and *tert*-butyl methyl ether is $(12.9 \pm 0.3) \times 10^{-5}\ s^{-1}$, which is about double that without H_3PO_2. Higher values of k_{dec} were found for acetone and *tert*-butyl methyl peroxide; the weighted mean is $(53.2 \pm 0.8) \times 10^{-5}\ s^{-1}$. One exceptional finding is the following: the rate of acetone production, normalized by [MTO], is 14 times higher with H_3PO_2 and its final concentration 45 times greater.

Discussion

O-Atom Transfer. Reaction 4 represents O-atom transfer from the alkyl hydroperoxide to the MDO. For the transfer to occur, the alkyl hydroperoxide coordinates to MDO, forming a transient intermediate. This species is analogous to those first formed when MTO combines with various E-OH species (H-OH, H-OOH, R-OH, etc.).[6,7,12,15]

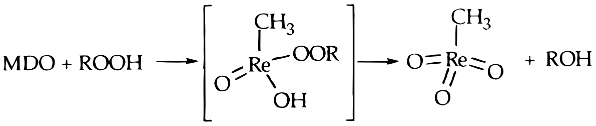

(9)

Equations 4 and 9 together account for rapid MTO buildup. One cannot say directly from the data whether the rate-controlling step is the coordination of the alkyl hydroperoxide or the breaking of the O−O bond. Given the high rate of MTO ligation reactions,[16] however, the rate-controlling step in reaction 9 seems most probably to be the breaking of the peroxide bond, as in the second step. The value of k_4 for *t*-BuOOH is only 7% larger than that for *t*-AmOOH, and the k_4 for H_2O_2 is slightly lower than that for either alkyl hydroperoxide. Two factors might contribute to these small differences in k_4: The more electron-donating R group provides a more nucleophilic peroxide anion, and thus a larger k_4, if the first step is rate-controlling. Also, *t*-AmOOH is slightly more sterically hindered than *t*-BuOOH, but this is at best a minimal determinant of the rate of MTO formation.

Kinetics of Decomposition of MTO and ROOH. The concurrent decomposition of MTO and H_2O_2 showed a $1/[H^+]$ kinetic dependence at $\mu = 0.05$ M. Methanol and perrhenate ions may be formed by one of these kinetically indistinguishable pathways:[6] (a) nucleophilic attack of HOO^-on MTO with $k_a = 2.03 \times 10^8$ L mol^{-1} s^{-1}

$$HOO^- + MeReO_3 \rightarrow [Me(O)_3Re{-}OOH]^- \rightarrow MeOH + ReO_4^-$$

(b) nucleophilic attack of OH^- on **A** with $k_b = 3.05 \times 10^9$ L mol^{-1} s^{-1}

$$OH^- + MeRe(O)_2(\eta^2\text{-}O_2) \rightarrow\rightarrow MeOH + ReO_4^-$$

(c) a reaction between H_2O_2 and $MTO{-}OH^-$, the conjugate base of MTO ($pK_a = 7.5$),[15] with $k_c = 3.1 \times 10^5$ L mol^{-1} s^{-1}

$$H_2O_2 + MeRe(O)_3(OH)^- \rightarrow\rightarrow MeOH + ReO_4^- + H_2O$$

These considerations guide us to an interpretation of the kinetic data for ROOH. The rate constant for the decomposition of MTO by *t*-BuOOH is also proportional to $1/[H^+]$, as shown in Figure 2. This could be interpreted by mechanism (a) or (c), but not by (b) since that would require the same rate constant for H_2O_2 and $RCMe_2OOH$. The experimental pH dependence can be expressed by the rate law given by eq 10.

$$v = \frac{k_s K_a [MTO][ROOH]}{[H^+]} \tag{10}$$

If mechanism (a) prevails, then $pK_a = 12.8$ for *t*-BuOOH and $k_s = 4.6 \times 10^8$ L mol^{-1} s^{-1}. If mechanism (c) provides the preferred pathway, then $pK_a = 7.5$ for $MTO{-}OH_2$[15] and $k_s = 2.3 \times 10^3$ L mol^{-1} s^{-1}. In eq 10, k_s represents the corresponding bimolecular rate constant for the mechanism indicated, k_a or k_c. The value of k_s is related to k_f (eq 8) by the relationship $k_f = k_s K_a$. Although credible arguments can be advanced for (a) over (c), it is useful to consider an alternative that renders the distinction moot.[17] This scheme involves a complex formed from MTO and ROOH in which the inductive effect of rhenium-

---

(15) Herrmann, W. A.; Fischer, R. W. *J. Am. Chem. Soc.* **1995**, *117*, 3223.

(16) Wang, W.-D.; Espenson, J. H. *J. Am. Chem. Soc.* **1998**, *120*, 11335.

(17) We are grateful to a reviewer for this suggestion.

(VII) enhances the acidity of the ROOH proton. This would lead to the intermediate, **I** (R = *t*-Bu, *t*-Am). Its different cleavage reactions would lead to the various products, as detailed in the next section.

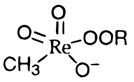

I

Decomposition of MTO and *t*-BuOOH. The proposed sequence of reactions for the concomitant decomposition of MTO and *t*-BuOOH under argon is presented in eqs 11−20. This is the simplest scheme we have been able to formulate to account for the products and the pH dependence.

$$\mathrm{MeReO_3} + t\text{-BuOOH} \rightarrow [\mathrm{Me(O)_3Re}\cdot t\text{-BuOOH}] \quad (11)$$

$$[\mathrm{Me(O)_3Re}\cdot t\text{-BuOOH}] \rightleftarrows [\mathrm{Me(O)_3Re{-}OOBu}\text{-}t]^- \; (=\mathbf{I}) + \mathrm{H^+} \quad (12)$$

$$\mathbf{I} \rightarrow t\text{-BuOMe} + \mathrm{ReO_4}^- \quad (13)$$

$$\mathbf{I} + \mathrm{H_2O} \rightarrow \mathrm{MeOH} + t\text{-BuOH} + \mathrm{ReO_4}^- \quad (14)$$

$$\mathbf{I} \rightarrow t\text{-BuO}^\bullet + \mathrm{Me}^\bullet + \mathrm{ReO_4}^- \quad (15)$$

$$t\text{-BuO}^\bullet \rightarrow \mathrm{Me_2CO} + \mathrm{Me}^\bullet \quad (16)$$

$$\mathrm{Me}^\bullet + t\text{-BuOOH} \rightarrow \mathrm{CH_4} + t\text{-BuOO}^\bullet \quad (17)$$

$$t\text{-BuO}^\bullet + t\text{-BuOOH} \rightarrow t\text{-BuOH} + t\text{-BuOO}^\bullet \quad (18)$$

$$2\,\mathrm{Me}^\bullet \rightarrow \mathrm{C_2H_6} \quad (19)$$

$$\mathrm{Me}^\bullet + t\text{-BuOO}^\bullet \rightarrow t\text{-BuOOMe} \quad (20)$$

In this scheme, very rapid coordination of *t*-BuOOH to MTO to form a neutral complex (eq 11) leads to the active intermediate **I** by acid ionization, eq 12. The partitioning of **I** among three reactions leads to the products. Dissociation of **I** forms *t*-BuOCH$_3$ and ReO$_4^-$, eq 13, cf. eq 2 with H_2O_2.[6] Formation of *t*-BuOMe from *t*-BuO$^\bullet$ and Me$^\bullet$ must happen in the transition state or solvent cage, because separated *t*-BuO$^\bullet$ and Me$^\bullet$ remain at concentrations too low for bimolecular recombination. Cleavage of **I** to ReO$_4^-$, *t*-BuO$^\bullet$, and CH$_3^\bullet$, eq 15, accounts for *t*-BuO$^\bullet$, and also for the CH$_3^\bullet$ that is derived from the methyl group on MTO. Intermediate **I** undergoes peroxide bond homolysis; furthermore, the C−Re bond breaks to give the stable ReO$_4^-$. There is precedent for the bond homolysis of a metal hydroperoxide. The scheme proposed for the hydroxylation of cycloalkanes by ROOH using $[\mathrm{Fe^{III}}_2\mathrm{O(TPA)_2(H_2O)_2}]^{4+}$ involves O−O bond homolysis.[18] Reaction 15 was written as a single step for simplicity of the scheme, but it is more likely that it happens sequentially. Indeed, eqs 13 and 15 may not be independent reactions.[17] The third mode by which **I** reacts is hydrolysis to methanol, *tert*-butyl alcohol, and perrhenate ions, eq 14.

Other steps, all very fast, complete the sequence: the *tert*-butoxyl radical and the methyl radical participate in a series of independently known steps, eqs 16−20, giving rise to acetone, methane, *tert*-butyl alcohol, ethane, and *tert*-butyl methyl peroxide. These products establish the involvement of methyl, alkoxyl, and alkylperoxyl radicals. The *t*-BuO$^\bullet$ radical continues the free-radical chemistry by undergoing β-scission form to acetone and the methyl radical, eq 16, $k_{16} = 1.4 \times 10^6$ s^{-1}.[19] The methyl radical then abstracts H$^\bullet$ from the *t*-BuOOH to give methane and *tert*-butylperoxyl radical, eq 17 ($k_{17} = 3 \times 10^4$ L mol^{-1} s^{-1}).[20] The *tert*-butoxyl radical, itself, can also abstract a hydrogen atom from *t*-BuOOH to give *tert*-butyl alcohol and *tert*-butylperoxyl radical, eq 18 ($k_{18} = 1.2 \times 10^6$ L mol^{-1} s^{-1}).[21] Another well-characterized reaction is the combination of two methyl radicals to form ethane, eq 19 ($k_{19} = 1.6 \times 10^9$ L mol^{-1} s^{-1}).[22]

The mixed dialkyl peroxide formed in the oxidation of hydrocarbons by ROOH has been taken to indicate free-radical involvement.[18,23] The dialkyl peroxide arises from the reaction of alkylperoxyl radicals and carbon centered radicals. By analogy, *tert*-butyl methyl peroxide is suggested to form from methyl radical and *tert*-butyl peroxyl radical, eq 20. This should be a diffusion-controlled reaction because both species are unstable radicals.[24]

Further evidence in support of the involvement of methyl radicals comes from experiments done in the presence of O_2. Two additional products were found, methyl hydroperoxide and formaldehyde. Methyl peroxyl radical is formed in the reaction between methyl radical and oxygen.[25] This radical could undergo a reaction analogous to eqs 17 and 18 to form methyl hydroperoxide and *t*-BuOO$^\bullet$: MeOO$^\bullet$ + *t*-BuOOH → MeOOH + *t*-BuOO$^\bullet$. Formaldehyde might then be a product of the bimolecular self-reaction of MeOO$^\bullet$: 2 MeOO$^\bullet$ → MeOH + CH$_2$O + O$_2$,[21] although a reviewer has noted that it might instead arise from Lewis acid (Re) catalyzed dehydration of MeOOH.

Consistent with the rate law and its [H$^+$]$^{-1}$ dependence, the partitioning reactions of **I** are, together, rate controlling. That option, which involves the breaking of covalent bonds, rather than a rate-controlling reaction between MTO and *t*-BuOO$^-$, is proposed for the formation of **I**, since precedents suggest the latter would be extremely rapid. According to that scheme, the general expression for the reaction rate is

$$\frac{\mathrm{d}[\mathbf{P}]}{\mathrm{d}t} = (k_{13} + k_{14} + k_{15})\frac{K_{11}[\mathrm{MTO}][\mathrm{ROOH}]}{1 + K_{11}[\mathrm{ROOH}]}\,\frac{k_{12}}{k_{12} + [\mathrm{H^+}]} \quad (21)$$

Because MTO was detected throughout the reaction and [Me(O)$_3$Re$\cdot$*t*-BuOOH] was not observed, $K_{11} < 10^2$ L mol^{-1}. Eigen and co-workers[26] report that the rate constant of proton association in an acid equilibrium reaction (k_{12}) is on the order of magnitude of 10^{10} L mol^{-1} s^{-1}. Therefore K_{12} is on the order of magnitude of 10^{-10} mol L^{-1}. With these assumptions and

---

[18] MacFaul, P. A.; Ingold, K. U.; Wayner, D. D. M.; Que, L., Jr. *J. Am. Chem. Soc.* **1997**, *119*, 10594.

[19] Erben-Russ, M.; Michel, C.; Bors, W.; Saran, M. *J. Phys. Chem.* **1987**, *91*, 2362.

[20] Bakac, A.; Wang, W.-D. *Inorg. React. Mech.* **1998**, *1*, 65.

[21] Bennett, J. E. *J. Chem. Soc., Faraday Trans.* **1990**, *86*, 3247.

[22] Hickel, B. *J. Phys. Chem.* **1975**, *79*, 1975.

[23] Nguyen, C.; Guajardo, R. J.; Mascharak, P. K. *Inorg. Chem.* **1996**, *35*, 6273.

[24] Kochi, J. K., Ed. *Free Radicals*; John Wiley and Sons: New York, 1973; Vol. 1.

[25] Suzuki, H.; Fukui, H.; Moro-oka, Y. in *The Role of Oxygen in Chemistry and Biochemistry*; Ando, W., Moro-oka, Y., Eds.; Elsevier: New York, 1988; pp 269−272.

[26] Barshop, B. A.; Wrenn, C. F.; Frieden, C. *Anal. Biochem.* **1983**, *130*, 134.

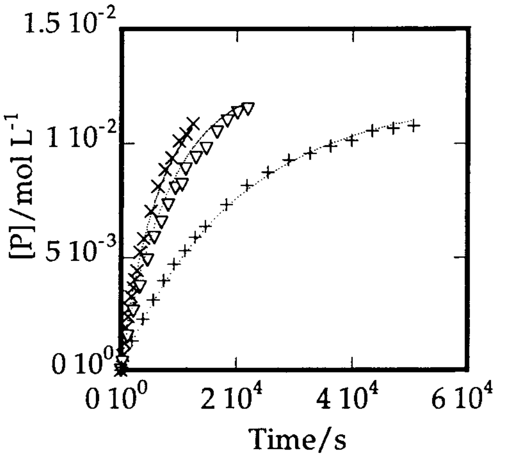

Figure 3. KinSim simulations (···) of the buildup in total organic products for the reaction of MTO at three concentrations of *t*-BuOOH, 0.60 M (×); 0.47 M (∇); and 0.20 M (+). The quantity on the *y* axis is [P] = ([(CH$_3$)$_2$CO] + [CH$_3$OH] + [*t*-BuOCH$_3$] + [*t*-BuOOCH$_3$])/M.

the experimental value for k_f of 7.4×10^{-5} s^{-1}, it follows that $k_{13} + k_{14} + k_{15} < 4 \times 10^3$ s^{-1}.

The reaction scheme consisting of eqs 11−20 was further explored by simulations using the KinSim program,[26−28] a routine for generating concentration−time curves given the initial concentrations and rate constants. The mathematical algorithms are based on Gear and Runge−Kutta calculations. Certain rate ratios were then optimized using the FitSim program.[29] In this manner, the agreement between the proposed reaction scheme and the experimental data could be tested. The experimental concentration−time curves for the decrease in MTO and increase in CH$_3$OH, (CH$_3$)$_2$CO, *t*-BuOCH$_3$, and *t*-BuOOCH$_3$ for three separate experiments ([MTO]$_0$ = 10 mM; [*t*-BuOOH]$_0$ = 200, 470, and 600 mM; [HOTf]$_0$ = 100 mM) were included as data in KinSim. Literature values for the known rate constants were used, except for the estimated value of k_{20} $\sim 2 \times 10^9$ mol L^{-1} s^{-1}, a choice not critical to the analysis. Rough estimates for the relative ratios of rate constants for steps 13−15 were calculated from the initial rates for product buildup. The unknown rate constants were fixed and varied, accordingly, in FitSim. The actual magnitudes of k_{13}, k_{14}, and k_{15} could not be established, only the ratios could: $k_{14}/k_{13} = 1.89$, $k_{15}/k_{13} = 1.61$, and $k_{15}/k_{14} = 0.85$ (reliability, ±20%). KinSim was used to simulate the total product buildup over time. The precision in measuring small concentrations of each product separately was rather low. Therefore, the buildup of the sum of product concentrations is used to represent the reaction course. Figure 3 shows that the simulated values correspond well with the experimental data, supporting the proposed mechanism.

Decomposition of MTO and *t*-AmOOH. To help us derive the scheme for the decomposition of methyltrioxorhenium and alkyl hydroperoxides, *t*-amyl hydroperoxide was employed on the basis of the observed products, the decomposition process using *t*-AmOOH goes by a sequence similar to that gone by the process using *t*-BuOOH. There will, of course, be some minor differences in the overall scheme. The *t*-AmO$^\bullet$ is known to undergo β-scission at a higher rate because it forms the more stable ethyl radical.[24,30] Also, additional gaseous products (e.g. propane and ethylene) are formed in the *t*-AmOOH case as a result of recombination of CH$_3^\bullet$ and CH$_3$CH$_2^\bullet$ and the self-reaction of CH$_3$CH$_2^\bullet$.

The chemical products in the reactions with *t*-BuOOH and *t*-AmOOH are formed in different relative and absolute yields, as can be seen from a comparison of the data in Tables 1 and 2. A precise mass balance was not feasible since products such as methane and ethane could not be determined on a comparable basis. Not only that, but certain products (e.g., MeOH and RMe$_2$COMe) form directly, whereas others (e.g., Me$_2$CO and RMe$_2$COOR) result from subsequent steps.

Smurova et al. recently reported that the addition of MTO to Ph(CH$_3$)$_2$COOH, cumyl hydroperoxide, in chlorobenzene resulted in the heterolytic decomposition of the hydroperoxide and that <1% of the process included radical pathways.[10] The chemistry of ROOH with MTO is much different in aqueous solution than in chlorobenzene. In fact, the aqueous chemistry of the decomposition of CH$_3$ReO$_3$ by *t*-BuOOH and *t*-AmOOH more closely resembles the decomposition of cumyl hydroperoxide by manganese(II) and -(III) acetylacetonates in chlorobenzene.[31]

Phosphoric Acid Formation. This product indicates a special mechanism operates with the ternary system (MTO, *t*-BuOOH, and H$_3$PO$_2$). Certain radicals react with H$_3$PO$_2$ and, especially, the H$_3$PO$_3$ formed from it. This general notion finds support from the greatly enhanced rate for acetone buildup and the substantial amount of acetone formed. These findings signal the generation of additional *t*-BuO$^\bullet$, the immediate precursor of acetone in eq 16.[19]

The methyl radical is postulated to abstract a hydrogen atom from H$_3$PO$_3$, eq 22, analogous to known reactions of H$^\bullet$, eq 23.[32]

$$\mathrm{CH_3^\bullet + H_3PO_3(or\ H_3PO_2) \rightarrow CH_4 + [P^\bullet(O)(OH)_2]\ (or\ [HP^\bullet(O)(OH)])} \tag{22}$$

$$\mathrm{H^\bullet + H_3PO_3(or\ H_3PO_2) \rightarrow H_2 + [P^\bullet(O)(OH)_2]\ (or\ [HP^\bullet(O)(OH)])} \tag{23}$$

The rate constants for k_{23} are 5.0×10^8 L mol^{-1} s^{-1} (H$_3$PO$_3$) and 4.2×10^9 L mol^{-1} s^{-1} (H$_3$PO$_2$).[31] Plausibly, the methyl radical abstracts H$^\bullet$ because the bond strengths of H$_2$ (434.1 kJ mol^{-1})[33] and CH$_4$ (435 kJ mol^{-1})[34] are virtually the same. There are, of course, differences in the rates of H-atom abstraction by H$^\bullet$ and CH$_3^\bullet$. For example, rate constants for α-hydrogen abstraction from alcohols are approximately 4 orders of magnitude greater with H$^\bullet$ than with CH$_3^\bullet$.[35,36]

The lower limit of k_{22} can be estimated from these data to be on the order of $>10^6$ mol L^{-1} s^{-1}, with an error of 1 order of magnitude, which is reasonable in that reaction 22 should be slower than reaction 23. With the long-chain approximation,[37] justified from the products formed, $k_{24} > 10^6$ L mol^{-1} s^{-1}. The phosphorus centered radicals generated in eq 22 are likely to

---

(27) Frieden, C. *Trends Biochem. Sci.* **1993**, *18*, 58.

(28) Frieden, C. *Methods Enzymol.* **1994**, *240*, 311.

(29) Zimmerle, C. T.; Frieden, C. *Biochem. J.* **1989**, *258*, 381.

(30) Walling, C. *Pure Appl. Chem.* **1967**, *15*, 69.

(31) Abdalla, A. A.-S.; Ivanchenko, P. A.; Solyanikov, V. M. *Kinet. Catal. (Transl. of Kinet. Katal.)* **1993**, *34*, 432.

(32) Muratbekov, M. B.; Seriev, A. S. *High Energy Chem. (Transl. of Khim. Vys. Energ.)* **1983**, *17*, 432.

(33) Cotton, F. A.; Wilkinson, G. *Advanced Inorganic Chemistry*, 5th ed.; John Wiley & Sons: New York, 1988.

(34) Lowry, T. H.; Richardson, K. S. *Mechanism and Theory in Organic Chemistry*, 3rd ed.; Harper Collins: New York, 1987.

(35) Thomas, J. K. *J. Phys. Chem.* **1967**, *71*, 1919.

(36) Smaller, B.; Avery, E. C.; Remko, J. R. *J. Chem. Phys.* **1971**, *55*, 2414.

(37) Espenson, J. H. *Chemical Kinetics and Reaction Mechanisms*, 2nd ed.; McGraw-Hill: New York, 1995.

attack the abundant hydroperoxide, eq 24, to form additional *tert*-butoxyl radicals that lead, in turn, to acetone,[19] eq 16, and to methyl radicals, further propagating the chain.

$$[\mathrm{P^{\bullet}(O)(OH)_2}]\ (\text{or}\ [\mathrm{HP^{\bullet}(O)(OH)}]) + t\text{-BuOOH} \rightarrow \mathrm{H_3PO_4}\ (\text{or}\ \mathrm{H_3PO_3}) + t\text{-BuO}^{\bullet} \quad (24)$$

Acknowledgment. This work was supported by the National Science Foundation Grant (CHE-9007283). We are grateful to Dr. Michael T. Ashby for supplying the CH_2DSn(*n*-butyl)$_3$ and to Dr. Andreja Bakac, Dr. Kamel Harrata, and Sahana Mollah for discussions and assistance.

IC9809052